Journal of Luminescence 198 (2018) 178–182

Contents lists available at ScienceDirect

Journal of Luminescence

journal homepage: www.elsevier.com/locate/jlumin

Hot carriers induced quenching of defects luminescence in Si doped AlN with Al core

Xiuhua Xie, Binghui Li*, Zhenzhong Zhang, Dezhen Shen

State Key Laboratory of Luminescence and Applications, Changchun Institute of Optics, Fine Mechanics and Physics, Chinese Academy of Sciences, Changchun 130033, People's Republic of China

A B S T R A C T

We investigated the spatial cathodoluminescence (CL) quenching of Si doped AlN/Al shell/core particles along the radial direction. The quenching characteristic position gradually shifts to a more central location with emission wavelength increasing. This effect is due to the transport process of hot electrons, which produced by Al-plasmon decay via Landau damping. In this transport process, donor levels (D_i) in AlN were partly occupied by hot electrons from Al core, which will reduce the quantum efficiency of recombination channel i (D_i to A_i). A phenomenological theory has been used to discuss carriers recombination dynamics processes.

1. Introduction

Hot carriers, produced by plasmon decay via Landau damping [1], have sparked considerable interest, recently, due to their broad applications in physical and chemical processes, including photodetection, femtochemistry, phase transitions and doping of two-dimensional materials [2–5]. The unique mechanisms of generation, relaxation, transport and ejection for hot carriers provide new opportunities for fundamental research [6]. Hitherto, hot carriers, ejected into nearby molecular and semiconductor systems, have been applied to research the energy conversion, photodetection and photocatalysis, successfully [2,7,8]. Essentially, these ejection processes are transitions of carriers from occupied to unoccupied states. Namely, it can be utilized to collect the information on the electronic structure of materials systems. Understanding the energy levels of point defects in the wide bandgap (E_g) semiconductors is crucial for achieving the effective and reliable conductive controlling [9,10]. As a very important member of wide E_g semiconductors, aluminum nitride (AlN), has plentiful defects energy levels, which are not understood well and controversial, at present [11–13].

In this letter, based on hot carriers in ejection and transport processes, we analyse the defect-related luminescence in Si-doped AlN by utilizing high spatial resolution cathodoluminescence (CL). Simultaneously, the accelerated electron beam of CL as an excitation source for aluminum (Al) plasmon. Then hot electrons are generated from Al core transport to the AlN sides. Due to the ultrafast timescale (10^{-15} to 10^{-13} s) for a plasmon transfer to a single electron-hole pair, Landau damping, compared with capture rates of carriers by defects (10^{-10} to 10^{-8} s) [6,14], unoccupied defect states will be occupied by hot carriers from Al core, which induced quenching of defects luminescence. The carrier recombination dynamics has been further discussed by using phenomenological theory.

2. Experiment

The sample under investigation in this study was grown in DCA-P600 (Finland) MBE system equipped with an oxford radio-frequency N_2 plasma source with ion removal control for active N atom, and solid-source effusion cells for Al and silicon (Si). Elemental Al (6 N5 grade), Si ($>$ 5000 Ω·cm) and N_2 gas with 6N grade were used as molecular beam sources. The beam equivalent pressure (i. e. molecular flux) was measured by using a nude ionization gauge, which working in front of the substrate. CL measurements were performed on an Attolight Rosa 4634 CL microscope, which tightly integrates a high numerical aperture (NA = 0.72) achromatic reflective lens within the objective lens of a field-emission-gun scanning electron microscope (FEG-SEM). The focal plane of the light lens matches the FEG-SEM optimum working distance. CL was spectrally resolved with a Czerny-Turner spectrometer (320 mm focal length, 150 grooves/mm grating) and measured with a UV–Vis sensor. The sample was inspected at low temperature (20 K) by employing a helium flow cryostat.

3. Results and discussion

Fig. 1(a) shows the scheme of the Si doped AlN with Al core fabrication procedure. Firstly, a Si doped AlN film was grown on the a-

* Corresponding author.
E-mail address: binghuili@163.com (B. Li).

https://doi.org/10.1016/j.jlumin.2018.02.045
Received 2 June 2017; Received in revised form 8 February 2018; Accepted 13 February 2018
Available online 14 February 2018
0022-2313/

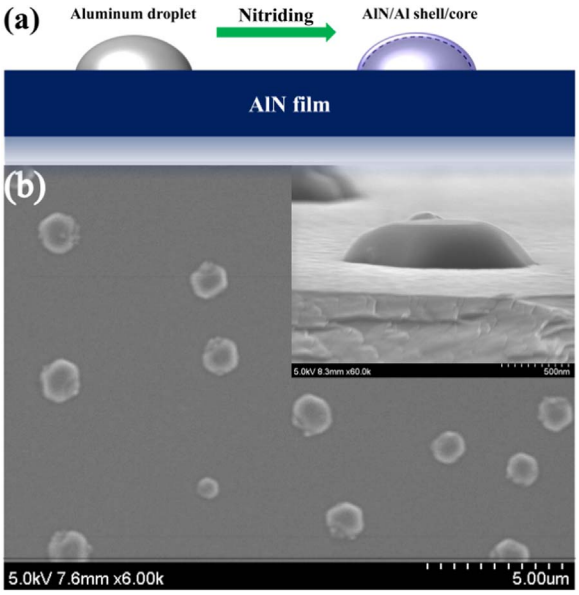

Fig. 1. (a) The scheme of the Si doped AlN with Al core fabrication procedure; (b) scanning electron microscopy images of Si doped AlN/Al shell/core arrays. The side view of one particle is shown in the inset.

plane sapphire with flux ratio Al/N ~1 at substrate temperature of 1000 °C. The flux ratio of Si/Al was about 1/800. Secondly, the beam flux of Al was slightly improved to make the Al/N > 1, then Al droplets doped with Si were formed on the top of AlN film [15,16]. Finaly, shutters of Al and Si were closed, while the N shutter maintains opening. Al droplets doped with Si were nitridated for 15 min at the growth temperature. Thus, a Si doped AlN shell (about 10 nm determined by the beam flux condition of N) was produced. Scanning electron microscopy (SEM) images of Si doped AlN/Al shell/core arrays were presented in Fig. 1(b). The AlN/Al shell/core has about 800 nm diameter and 240 nm high.

The scanning mode of CL electron beam at beam energy of 10 keV was illustrated in Fig. 2(a). The electron beam of CL was incident on the AlN film in the normal direction. The scanning range includes the entire area of SEM images. As shown in Fig. 2(b), the CL signal from the sample was composed of two broad bands centered at about 360 & 510 nm, hereafter referred to as blue and red band, respectively. No signal for exciton peak from AlN could be detected, due to the enormous quantity of defects. As can be seen in the superimposed monochromatic CL (MonoCL) signal map [(Fig. 2(c)] of blue and red band, these two bands were spatially uniform, except AlN/Al shell/core parts. CL intensities of blue and red band decreasing from the edge to the center of the shell/core particle, which suggesting some quenching mechanisms were existed.

For analysis the spatial CL quenching, carefully, MonoCL maps of a single particle for blue and red band with two emission shoulders (around 250–300 nm & 600–700 nm) were shown in Fig. 3. These four emission bands present different CL intensities distribution along the radial direction of the particle. Fig. 3(e) shows the dependence of normalized integrated CL intensities on the electron beam excitation position for the particle [sees dash line in the inset of Fig. 3(e)]. With the electron beam exciting point moving to the center of the particle, the emission of the red band was quenching at the edge of the particle, firstly. The quenching characteristic position, the position at which the integrated CL intensity starting drops, gradually shifts to a more central location with emission wavelength increasing. Note that the emission shoulder (around 600–700 nm) presents more slower decreasing of CL intensity with a constant trend near the center region, compare with other three emission bands, which indicating the different luminescence origin (see below for further discussion).

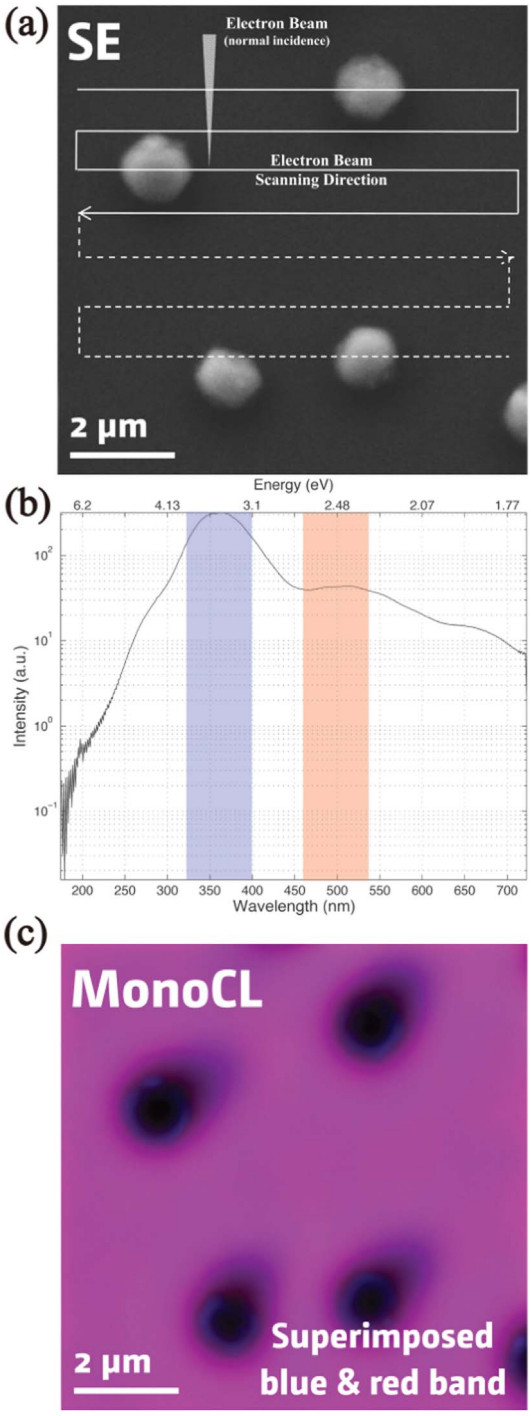

Fig. 2. (a) The scanning mode of CL electron beam; (b) the CL signal from sample; (c) the superimposed monochromatic CL signal map (two broad bands centered at 360 & 510 nm).

In order to illustrate the spatial CL quenching of the particle, main transitions in Si doped AlN/Al shell/core in conditions of CL have been constructed, as shown in Fig. 4. According to previous studies and their energy values [17–22], emission bands, centered at about 270 & 360 & 510 nm, have been assigned to Si and O related donors to Al vacancies (V_{Al}) related acceptors. While the emission band (centered at 670 nm) has been assigned to an internal transition associated with the V_{Al} defect. Therefore, Donor levels of D_1, D_2, D_3 have been assigned to 4Si:V_{Al}, Si_{Al} and O_N, respectively [12,17–20,22]. The O_N is come from undesirable inevitable contamination. Meanwhile, the acceptor level, A, has been assigned to V_{Al} related level, which was enhanced by Si doping

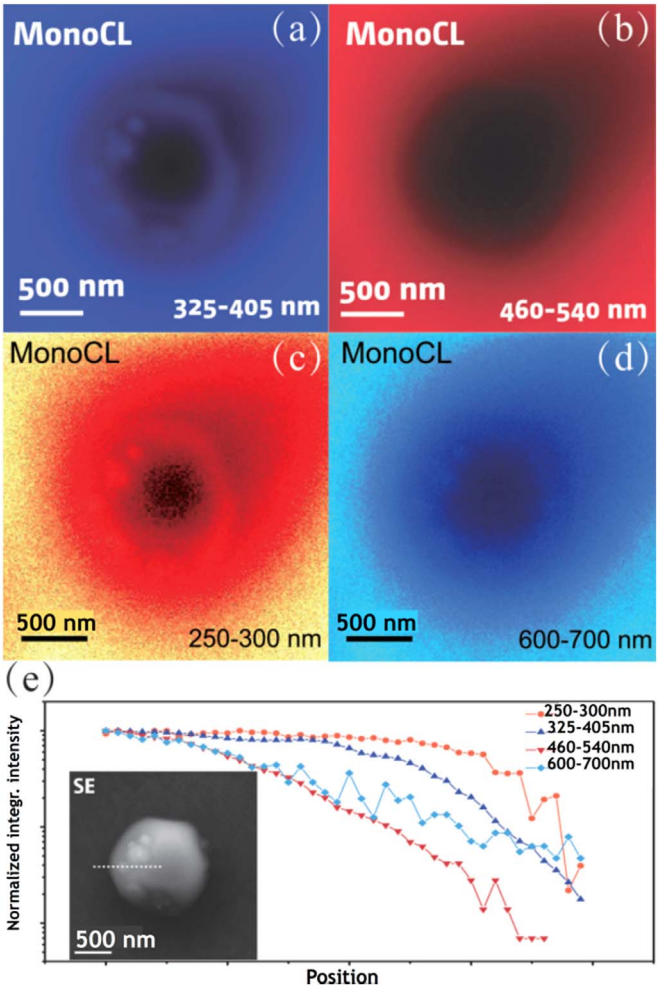

Fig. 3. Monochromatic CL images for a single particle (a) 325–405 nm (b) 460–540 nm (c) 250–300 nm & (d) 600–700 nm; (e) the dependence of normalized integrated CL intensities on the electron beam excitation position for the particle. The scanning direction is shown in the inset, white dash line.

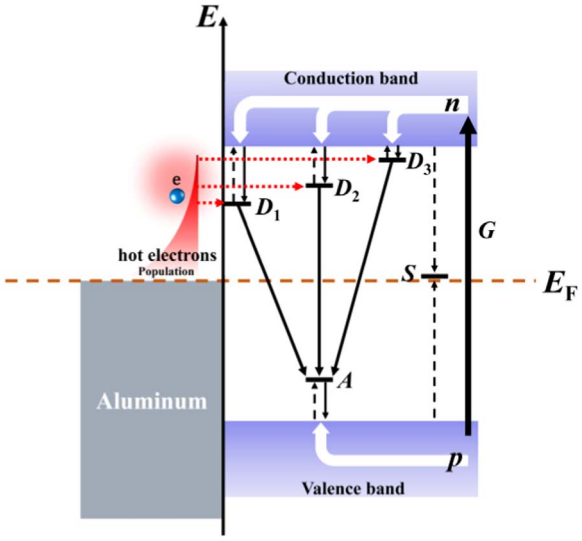

Fig. 4. Main transitions of carriers in Si doped AlN/Al shell/core in conditions of CL. The red dash arrows indicate transfer processes of hot electrons.

[23,24]. It is useful to clarify that there should be three type acceptor levels, A_i (i = 1, 2, 3), which correspond to the D_i to A_i recombination. Due to lack sufficient evidence from previous reports, for simplicity in Fig. 4, only one type acceptor level has been labeled. Besides, there is the third type of defects (S), nonradiative recombination centers. Irradiation with an electron beam creates electron-hole pairs with rate G. Nonequilibrium carriers relax quickly to the valence-band maximum (for holes) and the conduction-band minimum (for electrons), respectively. And then, electrons are captured by positively charged D_i (i = 1, 2, 3), while holes are captured by negatively charged A. These capture transitions are on the timescale of 10^{-10} to 10^{-8} s and nonradiative. Meanwhile, parts of nonequilibrium carriers were quickly captured by S centers. Finally, radiative transitions caused by donor-acceptor-pair (DAP) recombination are produced. Moreover, taking into account aluminum plasmonics excited by CL electron beam under enough penetration depths (to penetrate 10 nm AlN shell), hot electrons created by plasmon decay via Landau damping, with energies ranging from the Fermi level E_F up to $E_F + \hbar\omega_p$ [2,6,25], where $\hbar\omega_p$ is the plasmon resonances energy, will transfer into donor levels (D_i) in the AlN, as illustrated in Fig. 4, the red dash arrows. This kind of transfer process of hot electrons will affect the quantum efficiency of matched D_i to A recombination (see below for further discussion). As can been seen in the Fig. 5, we simulated numerous electron trajectories in our Si doped AlN/Al shell/core under 10 keV acceleration voltages using a Monte Carlo method (software "CASINO", available online) [26]. At the edge of the particle, less quantity of accelerated electrons penetrate into the Al core, where lower energy diameter-mode plasmon resonances were excited [27]. Hence, some of D_1 states will be occupied by hot electrons with lower energy, firstly. With the incidence (θ) decreasing, the electron beam of CL moving close to the top of the AlN/Al particle, as shown in Fig. 5, more quantities of accelerated electrons penetrate into the Al core, then higher energy plasmon resonances, radius-mode, become dominated [28]. Thus, higher energy level states, D_3, will be occupied. It is consistent with the quenching characteristic position gradually shifts to a more central location with emission wavelength increasing. In addition, hot carriers can also remain trapped inside the Al core, following rapid relaxation processes [29], and cause local heating of AlN/Al shell/core. Under the local heating, induced by the internal decay of hot carriers, the internal transition associated with the V_{Al} defect (centered at 670 nm) will be gradually replaced by a nonradiative recombination process, in which the V_{Al} defects were thermal excited to the cross-over point of the adiabatic potentials of its excited and ground states [30].

Here, we use a phenomenological theory to further discuss the recombination of nonequilibrium carriers with hot electrons transport. Firstly, considering the normal recombination process, after accelerated electrons excitation, nonequilibrium electrons (holes) are captured by donors (acceptors) and nonradiative recombination centers. Due to the low temperature (20 K in this work), the thermal activation (bound electrons or holes return to the conduction band or valence band, respectively) can be ignored. Taking into account all capture processes, the steady-state equation for the electron concentration (n) in the conduction band can be expressed as

$$\frac{\partial n}{\partial t} = G - \sum_{i=1}^{3} C_{ni} N_{Di}^{+} n - C_{nS} N_S n = 0. \tag{1}$$

where C_{ni} is the electron-capture coefficient for the D_i and N_{Di}^{+} is the concentration of positively charged D_i. C_{nS} and N_S are the average electron-capture coefficient and the concentration of S, respectively.

Equally, for holes concentration (p) in the valence band, the steady-state equation can be expressed in the form

$$\frac{\partial p}{\partial t} = G - \sum_{i=1}^{3} C_{pi} N_{Ai}^{-} p - C_{pS} N_S p = 0. \tag{2}$$

where C_{pi} is the hole-capture coefficient for A_i; N_{Ai}^{-} is the concentration

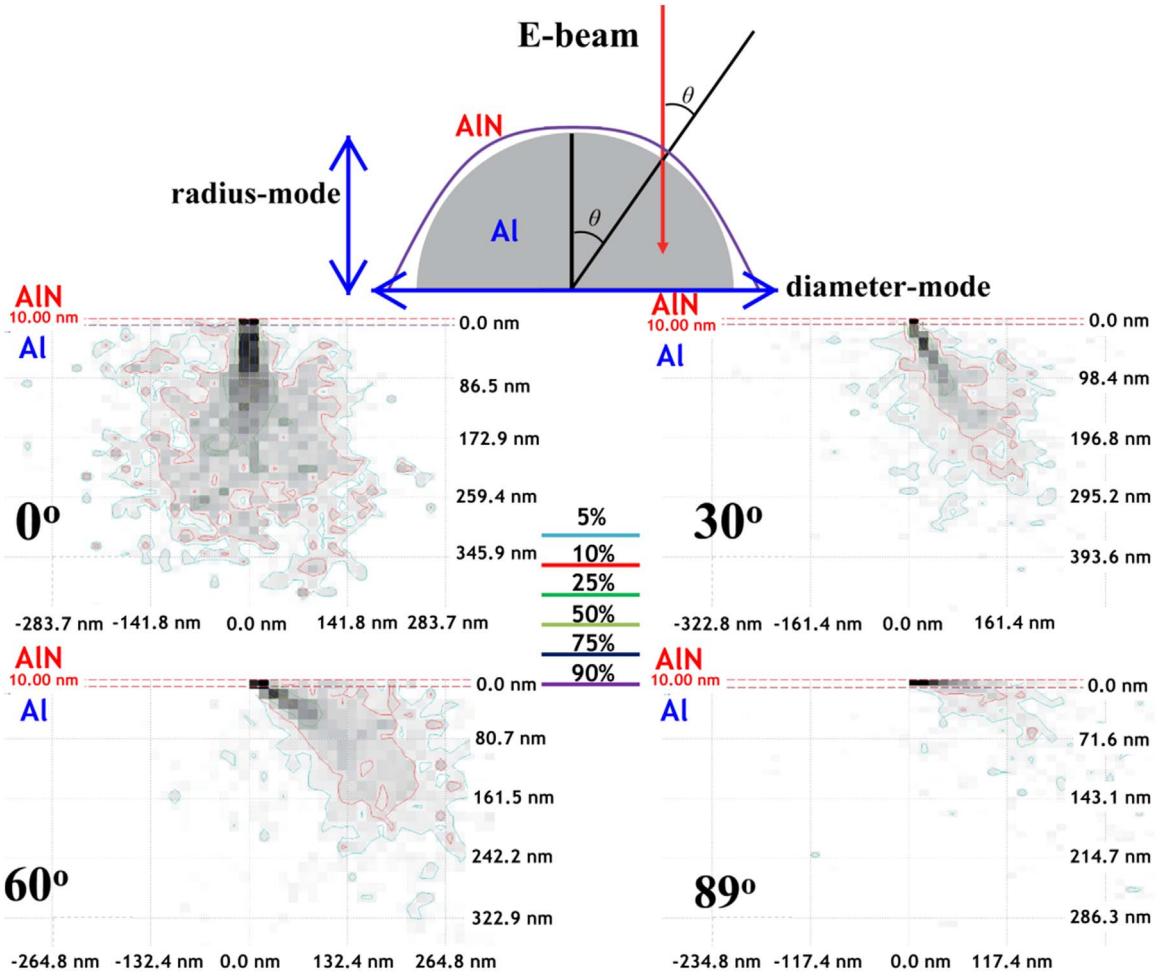

Fig. 5. Contour plot of the electron energy in our Si doped AlN/Al shell/core simulated by the Monte Carlo method under 10 keV acceleration voltages and different incident angles.

of negatively charged A_i; C_{pS} is the average hole-capture coefficient of S.

The next step involves considering hot electrons transport process. When hot electrons transfer into the D_i in the AlN, the capture rate of nonequilibrium electrons in conduction band, $C_{ni}N_{Di}^{+}n$, can be changed as $C_{ni}(N_{Di}^{+} - n_i^{hot})n$, where n_i^{hot} is the concentration of hot electrons transferred into the D_i. Here, nonradiative centers have been assumed in the middle region of the bandgap. Thus, under the charge conservation, the rate $C_{ns}N_sn$, electrons captured by S, is equal to $C_{ps}N_sp$, the rate of holes captured by S. Then, by solving resulting Eqs. (1), (2) simultaneously, the capture rate for holes can be determined, $C_{pi}N_{Ai}^{-}p = C_{ni}N_{Di}^{+}n$. While taking into account hot electrons transport process, $C_{pi}N_{Ai}^{-}p = C_{ni}(N_{Di}^{+} - n_i^{hot})n$.

Because the recombination efficiency of channel i (D_i to A_i) is proportional to the specific A_i holes capture rate, the quantum efficiency of recombination channel i, η_i, is determined by the ratio of the capture rate of holes for the recombination channel i to the total capture rate of holes,

$$\eta_i = \frac{C_{pi}N_{Ai}^{-}p}{C_{pS}N_Sp + \sum_{i=1}^{3} C_{pi}N_{Ai}^{-}p}. \quad (3)$$

As mentioned above, when hot electrons transport process taking placed, own to $C_{ni}(N_{Di}^{+} - n_i^{hot})n < C_{ni}N_{Di}^{+}n$, the η_i^{*} (quantum efficiency of recombination channel i with D_i occupied partly by hot electrons) is smaller than the normal (without hot electrons transitions).

4. Conclusion

In conclusion, the spatial quenching of defects-related luminescence in Si doped AlN/Al shell/core particles were examined. The unique quenching performance, which characteristic quenching position depends on the emission wavelength, was explained by taking into account Al-plasmon induced hot electrons transport process. By using a phenomenological theory, the reducing of quantum efficiency of recombination channel i with D_i occupied partly by hot electrons was well discussed.

Acknowledgments

The authors gratefully acknowledge support from the National Natural Science Foundation of China (NSFC) under Grant No. 61376054 and 61505200. The authors thank Attolight for their assistance with CL measurements.

References

[1] X.G. Li, D. Xiao, Z.Y. Zhang, Landau damping of quantum plasmons in metal nanostructures, New J. Phys. 15 (2013) 023011.
[2] M.W. Knight, H. Sobhani, P. Nordlander, N.J. Halas, Photodetection with active optical antennas, Science 332 (6030) (2011) 702–704.
[3] J. Gavnholt, A. Rubio, T. Olsen, K.S. Thygesen, J. Schiotz, Hot-electron-assisted femtochemistry at surfaces: a time-dependent density functional theory approach, Phys. Rev. B 79 (2009) 195405.
[4] Y.M. Kang, S. Najmaei, Z. Liu, Y.J. Bao, Y.M. Wang, X. Zhu, N.J. Halas, P. Nordlander, P.M. Ajayan, J. Lou, Z.Y. Fang, Plasmonic hot electron induced structural phase transition in a MoS_2 monolayer, Adv. Mater. 26 (37) (2014) 6467–6471.
[5] Z.Y. Fang, Y.M. Wang, Z. Liu, A. Schlather, P.M. Ajayan, F.H.L. Koppens, P. Nordlander, N.J. Halas, Plasmon-induced doping of graphene, ACS Nano 6 (11) (2012) 10222–10228.

[6] M.L. Brongersma, N.J. Halas, P. Nordlander, Plasmon-induced hot carrier science and technology, Nat. Nanotechnol. 10 (1) (2015) 25–34.
[7] I. Thomann, B.A. Pinaud, Z.B. Chen, B.M. Clemens, T.F. Jaramillo, M.L. Brongersma, Plasmon enhanced solar-to-fuel energy conversion, Nano Lett. 11 (8) (2011) 3440–3446.
[8] J.S. DuChene, B.C. Sweeny, A.C. Johnston-Peck, D. Su, E.A. Stach, W.D. Wei, Prolonged hot electron dynamics in plasmonic-metal/semiconductor heterostructures with implications for solar photocatalysis, Angew. Chem. Int. Ed. 53 (30) (2014) 7887–7891.
[9] C. Freysoldt, B. Grabowski, T. Hickel, J. Neugebauer, G. Kresse, A. Janotti, C.G. Van de Walle, First-principles calculations for point defects in solids, Rev. Mod. Phys. 86 (1) (2014) 253–305.
[10] S.J. Pearton, J.C. Zolper, R.J. Shul, F. Ren, GaN: processing, defects, and devices, J. Appl. Phys. 86 (1) (1999) 1–78.
[11] C. Stampfl, C.G. Van de Walle, Theoretical investigation of native defects, impurities, and complexes in aluminum nitride, Phys. Rev. B 65 (15) (2002) 155212.
[12] D.F. Hevia, C. Stampfl, F. Vines, F. Illas, Microscopic origin of n-type behavior in Si-doped AlN, Phys. Rev. B 88 (8) (2013) 085202.
[13] N.T. Son, M. Bickermann, E. Janzen, Shallow donor and DX states of Si in AlN, Appl. Phys. Lett. 98 (9) (2011) 092104.
[14] M.A. Reshchikov, Temperature dependence of defect-related photoluminescence in III-V and II-VI semiconductors, J. Appl. Phys. 115 (1) (2014) 012010.
[15] G. Koblmueller, R. Averbeck, L. Geelhaar, H. Riechert, W. Hosler, P. Pongratz, Growth diagram and morphologies of AlN thin films grown by molecular beam epitaxy, J. Appl. Phys. 93 (12) (2003) 9591–9596.
[16] V. Lebedev, F.M. Morales, H. Romanus, S. Krischok, G. Ecke, V. Cimalla, M. Himmerlich, T. Stauden, D. Cengher, O. Ambacher, The role of Si as surfactant and donor in molecular-beam epitaxy of AlN, J. Appl. Phys. 98 (9) (2005) 093508.
[17] B.E. Gaddy, Z. Bryan, I. Bryan, R. Kirste, J.Q. Xie, R. Dalmau, B. Moody, Y. Kumagai, T. Nagashima, Y. Kubota, T. Kinoshita, A. Koukitu, Z. Sitar, R. Collazo, D.L. Irving, Vacancy compensation and related donor-acceptor pair recombination in bulk AlN, Appl. Phys. Lett. 103 (16) (2013) 161901.
[18] Q.M. Yan, A. Janotti, M. Scheffler, C.G. Van de Walle, Origins of optical absorption and emission lines in AlN, Appl. Phys. Lett. 105 (11) (2014) 111104.
[19] T. Koyama, M. Sugawara, T. Hoshi, A. Uedono, J.F. Kaeding, R. Sharma, S. Nakamura, S.F. Chichibua, Relation between Al vacancies and deep emission bands in AlN epitaxial films grown by NH_3-source molecular beam epitaxy, Appl. Phys. Lett. 90 (24) (2007) 241914.
[20] S.F. Chichibu, T. Onuma, K. Hazu, A. Uedono, Major impacts of point defects and impurities on the carrier recombination dynamics in AlN, Appl. Phys. Lett. 97 (20) (2010) 201904.
[21] T. Onuma, T. Shibata, K. Kosaka, K. Asai, S. Sumiya, M. Tanaka, T. Sota, A. Uedono, S.F. Chichibu, Free and bound exciton fine structures in AlN epilayers grown by low-pressure metalorganic vapor phase epitaxy, J. Appl. Phys. 105 (2) (2009) 023529.
[22] B. Bastek, F. Bertram, J. Christen, T. Hempel, A. Dadgar, A. Krost, Analysis of point defects in AlN epilayers by cathodoluminescence spectroscopy, Appl. Phys. Lett. 95 (3) (2009) 032106.
[23] E. Monroy, J. Zenneck, G. Cherkashinin, O. Ambacher, M. Hermann, M. Stutzmann, M. Eickhoff, Luminescence properties of highly Si-doped AlN, Appl. Phys. Lett. 88 (7) (2006) 071906.
[24] Q. Wu, N. Liu, Y.L. Zhang, W.J. Qian, X.Z. Wang, Z. Hu, Tuning the field emission properties of AlN nanocones by doping, J. Mater. Chem. C 3 (5) (2015) 1113–1117.
[25] A. Manjavacas, J.G. Liu, V. Kulkarni, P. Nordlander, Plasmon-Induced Hot Carriers in Metallic Nanoparticles, ACS Nano 8 (8) (2014) 7630–7638.
[26] Available "CASINO" online at 〈http://www.gel.usherbrooke.ca/casino/〉.
[27] C. Langhammer, M. Schwind, B. Kasemo, I. Zoric, Localized Surface Plasmon Resonances in Aluminum Nanodisks, Nano Lett. 8 (5) (2008) 1461–1471.
[28] J. Martin, J. Plain, Fabrication of aluminium nanostructures for plasmonics, J. Phys. D: Appl. Phys. 48 (18) (2015) 184002.
[29] G. Baffou, R. Quidant, C. Girard, Heat generation in plasmonic nanostructures: influence of morphology, Appl. Phys. Lett. 94 (15) (2009) 153109.
[30] A. Alkauskas, Q.M. Yan, C.G. Van de Walle, First-principles theory of nonradiative carrier capture via multiphonon emission, Phys. Rev. B 90 (2014) 075202.